energies

MDPI

Article

Reducing Traction Energy Consumption with a Decrease in the Weight of an All-Metal Gondola Car

Maryna Bulakh [1,*], Leszek Klich [1], Oleksandra Baranovska [2], Anastasiia Baida [3] and Sergiy Myamlin [4]

[1] Faculty of Mechanics and Technology, Rzeszow University of Technology, 37-450 Stalowa Wola, Poland
[2] Faculty of Political Science and Journalism, University of Maria Curie-Skłodowska, 20-612 Lublin, Poland
[3] Faculty of Law, Canon Law and Administration, The John Paul II Catholic University of Lublin, 20-950 Lublin, Poland
[4] Department of Electrical Power Engineering, Electrical Engineering and Electromechanics, Ukrainian State University of Railway Transport, 61050 Kharkiv, Ukraine
* Correspondence: m.bulakh@prz.edu.pl

Abstract: The paper presented studies on reducing traction energy consumption with a decrease in the weight of an all-metal gondola car. Based on the proposed mathematical criterion, a new form of a blind floor was obtained, which makes it possible to reduce the weight of an all-metal gondola car. The aim of the paper was to reduce traction energy consumption with a decrease in the weight of an all-metal gondola car. For an all-metal gondola car with a modified form of a blind floor, strength studies were performed based on the finite element method. The equivalent stresses of the blind floor of an all-metal gondola car were 140.6 MPa, and the equivalent strains were 7.08×10^{-4}. The margin of safety of the blind floor of an all-metal gondola car was 1.57. The weight of an all-metal gondola car with a modified form of a blind floor was reduced by 5.1% compared to a typical all-metal gondola car. For an all-metal gondola car with a modified form of a blind floor, a comparison was made of the traction energy consumption with typical all-metal gondola cars. Traction energy consumption with empty all-metal gondola cars were reduced by 2.5–3.1%; with loaded all-metal gondola cars by 2.4–7.3%, depending on the travel time interval.

Keywords: traction energy consumption; all-metal gondola car; rail transport; blind floor; weight; lightweighting

check for updates

Citation: Bulakh, M.; Klich, L.; Baranovska, O.; Baida, A.; Myamlin, S. Reducing Traction Energy Consumption with a Decrease in the Weight of an All-Metal Gondola Car. *Energies* **2023**, *16*, 6733. https://doi.org/10.3390/en16186733

Academic Editor: Giovanni Lutzemberger

Received: 10 August 2023
Revised: 3 September 2023
Accepted: 20 September 2023
Published: 21 September 2023

Copyright: © 2023 by the authors. Licensee MDPI, Basel, Switzerland. This article is an open access article distributed under the terms and conditions of the Creative Commons Attribution (CC BY) license (https://creativecommons.org/licenses/by/4.0/).

1. Introduction

Rail transport is an important economic sector in the world. To ensure the uninterrupted delivery of goods and people, the proper level of traffic safety and environmental safety [1,2] must be ensured.

Traffic safety on railways affects the speed of delivery of goods and passengers. The traction energy consumption has an impact on the competitiveness of rail transport.

Every day the need for freight and passenger transportation increases. At the same time, requirements have been made to reduce traction energy consumption. To reduce the traction energy consumption, various solutions have been proposed, for example [3–5]. Thus, in [3], on the basis of a simulation model of optimal train control, an assessment has been made of strategies for reducing traction energy consumption. However, this work has been related to metro systems.

In works [4–7], to reduce the energy consumption of an electric locomotive, the traction power control method and dynamic programming was used. The presented methods have been limited by the conditions of use. In works [8,9], energy-saving approaches in operation were considered. These works have been limited to use in urban rail transport systems. In works [10–15], the optimization of thrust energy was performed. However, these works have been limited to use in metro lines. In the works of [16–22], an energy-efficient strategy for driving trains was presented. These works have been limited by the conditions of use.

In the works of [23–25], fuzzy logic has been used to obtain optimal energy values. Alas, these works have been also limited by the conditions of use.

In the works of [26–30], for railway networks, a solution was given to reduce the use of traction energy. These works have been limited by the conditions of use.

In the works of [31–34], the use of traction energy was considered taking into account climatic conditions. These works have been limited by the climatic conditions of use.

However, all known solutions are narrowly focused, which does not allow them to be massively applied to all railway networks to reduce traction energy consumption.

The theme of lightweighting to obtain savings in consumption is very important in the transport sector, especially in the automotive sector. In the vehicular sector, the result of the lightweighting is influenced by the various parameters of the vehicle itself [35], use of lightweight materials for automobiles [36,37], including composite material [38]. Lightweighting creates have been discussed from a structural engineering standpoint [39].

In the rail transport sector, there is a similar trend as in the automotive sector.

In the works of [40–44], it was presented the results on the optimal lightweighting of rail vehicles using composite materials. However, in all works, composite materials have been used in passenger cars. In addition, the use of composite materials in gondola cars [45–47] has been complicated by the manufacturing technology.

In the works of [48–51], a constructive change of axles and wheelset was proposed to reduce the weight of a gondola car. These works do not present the results of implementation in practice.

Undoubtedly, research work on reducing the weight of gondola cars exists. However, studies on the effect of reducing the weight of gondola cars on the traction energy consumption have not been identified.

To solve the problem of reducing traction energy consumption on all railway networks, it is the use of engineering solutions to reduce the weight of gondola cars. "Gondola car" is an open part of a train that is used for transporting heavy goods. The meaning of this proposal is not to reduce the loading of gondola cars, but, namely, to reduce the weight of the gondola car to increase its carrying capacity.

This proposal to reduce traction energy consumption while reducing the weight of the gondola car is simple. However, reducing the weight of gondola car is not easy.

On the railways, different models of gondola cars have been used for freight transportation. The design of new generation gondola cars should be more durable, have a lower weight, increased carrying capacity and cost-effectiveness in operation.

This work has been limited to the study of an all-metal gondola car with a blind floor. Thus, the traction energy consumption has been studied depending on the weight of an all-metal gondola car with a blind floor.

The aim of the work was to reduce the traction energy consumption with a decrease in the weight of an all-metal gondola car.

2. Materials and Methods

2.1. Traction Energy Consumption Depending on the Weight of a Gondola Car

Traction energy consumption (E) can be set by the following function:

$$E = \widetilde{J}(\, W, L, I), \tag{1}$$

where W is the gross weight of a train;

L is the length of the section;

I is the interval of train movement on the section.

The gross weight of a train is determined by the equation:

$$W = W_l + \sum_{i=1}^{n} W_i^{gc} + \sum_{i=1}^{n} W_i^{c}\,, \qquad i = 1, \ldots, n, \tag{2}$$

where W_l is the weight of the locomotive;

W_i^{gc} is weight of the i-th gondola car;
W_i^c is weight of the i-th cargo;
n is the number of gondola cars.

Since the aim of the work was to decrease in the weight of an all-metal gondola car, the value W_i^{gc} can be changed in Equation (2). Accordingly, the values W_l and W_i^c will be constant.

Since the emphasis is on the weight of the gondola car, then the function (1) will take the form:

$$E = \widetilde{J}(\, W_i^{gc}, L, I), \tag{3}$$

for which it is necessary to determine the functions $W_i^{gc} \in \Omega(x, y, \pi);\ L \in \Omega^*;\ I \in \Omega^*$, at which the minimum traction energy consumption is achieved:

$$\mathbf{min}\ E = \min_{W^{gc} \in \Omega}\ \max_{L, I \in \Omega^*}\ \widetilde{J}(\, W_i^{gc}, L, I), \tag{4}$$

where Ω is the class of distribution functions of the step-type;
Ω^* is a set of the step-type distribution functions.

If we assume that the energy consumption proceeds according to a distributed law $G(x)\ \in \Omega^*$, and assume that there are functions of the numerator A and denominator B of the function $\widetilde{J}(\, W_i^{gc}, L, I)$, as well as their extremes, then the minimum of the function (4) can be achieved for any fixed $G(x)$, therefore:

$$\mathbf{min}\ E = \min_{W_i^{gc} \in \Omega}\ \max_{L, I \in \Omega^*}\ \widetilde{J}(\, W_i^{gc}, L, I) = \min_{0 \le v \le \infty}\ \max_{0 \le x \le \infty} \frac{\sum\limits_{i=0}^{n} A(x, v, y_i + 0)\ \Delta\pi_i}{\sum\limits_{i=0}^{n} B(x, v, y_i + 0)\ \Delta\pi_i}, \tag{5}$$

where x, v are parameters of the step-type function;
y_i is half interval of the i-th interval;
$\Delta\pi_i = \pi_{i+1} - \pi_i$ is exactly one step of parameter π_i.
The extremum of the function $\widetilde{J}(\, W_i^{gc}, L, I)$ is reached on functions of the step-type.

A decrease the traction energy consumption (Equation (3)) will occur with a decrease in the weight of the gondola car.

To reduce the weight of the gondola car, it is necessary to consider the design of the gondola car and propose a solution to this problem.

A typical cross-section of the body of an all-metal gondola car with a blind floor can be represented as follows (Figure 1).

A blind floor (3) of Figure 1 reduces stresses in the load-bearing elements of the body frame of an all-metal gondola car. For such gondola cars, there is a margin for reducing the mass of frame elements. In this case, the blind floor is subjected to the simultaneous action of vertical and horizontal loads. The action of a vertical load on a blind floor leads to a deflection, the magnitude of which determines the appearance of bending moments from a horizontal load and additional stresses. Also, additional bending moments can be caused by the initial curvature of the load-bearing elements of the body of an all-metal gondola car.

The blind floor of all-metal gondola cars is made of a rolled sheet, in some cases, the sheet is additionally stamped to form protrusions—corrugations—in order to increase strength, and materials that have a lower specific gravity and greater strength are also used.

2.2. Theoretical Preconditions for Reducing the Weight of an All-Metal Gondola Car

Theoretical preconditions for reducing the weight of an all-metal gondola car are as follows.

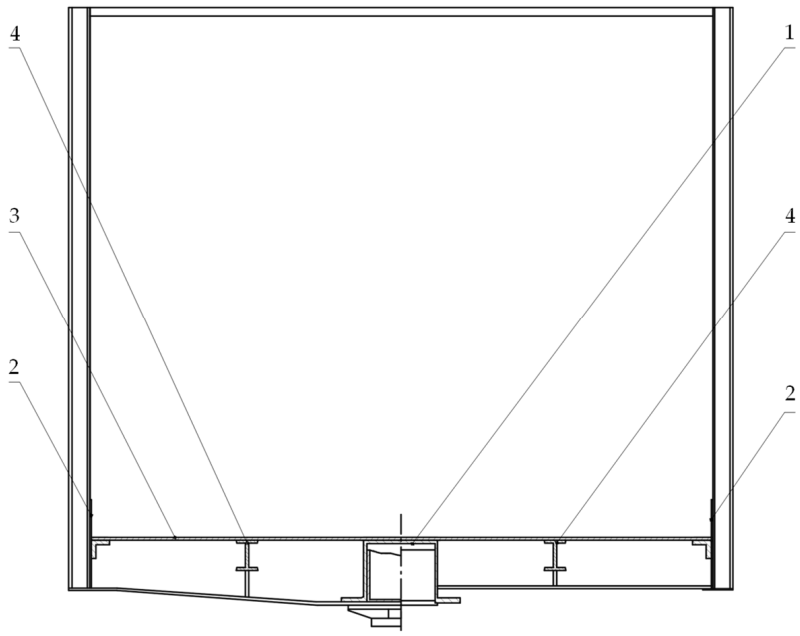

Figure 1. A typical cross-section of the body of an all-metal gondola car with a blind floor: (1) Spinal beam; (2) bottom side panel; (3) blind floor; (4) cross-beam.

Figure 2 shows a model of an all-metal gondola car with a blind floor and the action of a point load Q along the Z axis.

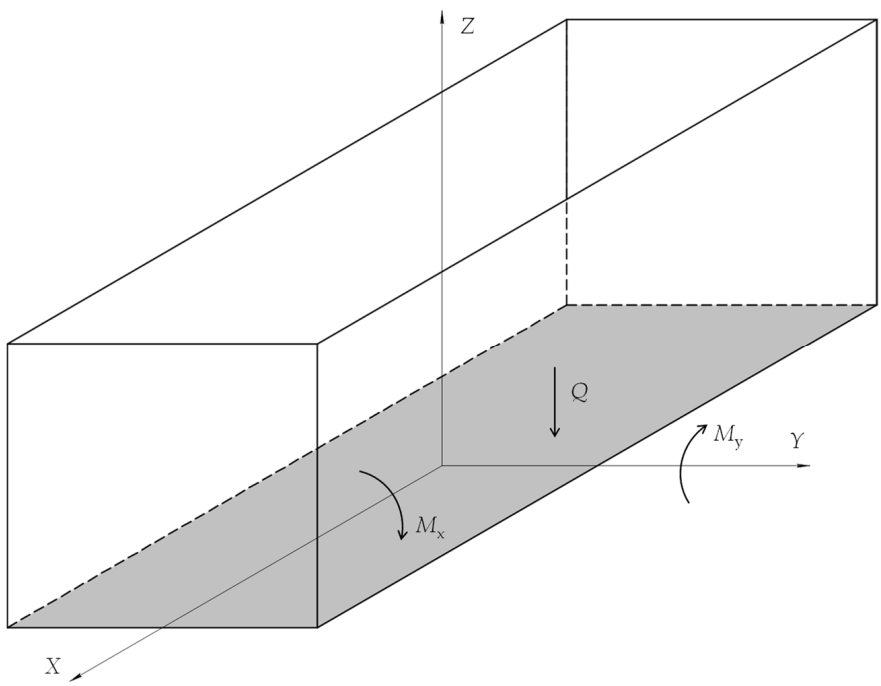

Figure 2. Model of an all-metal gondola car with a blind floor and the action of a point load Q along the Z axis (M_x and M_y are the bending moments that act about the X and Y axes, respectively).

Let us consider the action of a point load Q on the blind floor of an all-metal gondola car. A point load Q gives rise to bending moments M_x and M_y.

The maximum stresses ($\sigma_{\mathbf{max}}$) in the blind floor of an all-metal gondola car from the strength condition can be calculated by the equation:

$$\sigma_{\mathbf{max}} = \frac{Q_z}{A_{bf}} + \frac{M_x}{S_x} + \frac{M_y}{S_y} \leq [\sigma], \tag{6}$$

where A_{bf} is the area of the longitudinal section of the blind floor;

M_x, M_y are the bending moments that act about the X and Y axes, respectively;

S_x, S_y are the elastic section modulus about the X and Y axes, respectively;

$[\sigma]$ is the allowable stress for the material blind floor of an all-metal gondola car.

Based on function (3), in order to reduce the maximum stresses in the blind floor of an all-metal gondola car, it is necessary to increase the cross-sectional area A and the elastic section modulus S_x, S_y. This can be achieved by changing the shape of the blind floor of an all-metal gondola car.

By reducing the values of maximum stresses, the weight of the blind floor of an all-metal gondola car can be reduced.

Let us formulate the criterion for the shape of the blind floor of an all-metal gondola car:

$$J\left(A, W_x, W_y, W^{gc}\right) = \begin{cases} A \to \mathbf{max}; \\ S_x \to \mathbf{max}; \\ S_y \to \mathbf{max}; \\ W^{gc} \to \mathbf{min}. \end{cases}, \tag{7}$$

with the initial conditions:

$$A = A_0;\ W^{gc} = W_0^{gs}.$$

Using the minimax criterion, we write the criterion for the shape of the blind floor of an all-metal gondola car in the following form:

$$\widehat{J}_0 = \underset{W^{gc}\in\Omega}{\mathbf{min}}\ \underset{A,S_x,S_y\in\Omega}{\mathbf{max}}\ J_0\left(A,\ S_x,\ S_y,\ W^{gc}\right), \tag{8}$$

The extremum of the function (8) will be on the steps of the functions.

2.3. Method for Studying Stresses and Strains of the Blind Floor of an All-Metal Gondola Car Subsection

Stress and strains studies were carried out for the blind floor of an all-metal gondola car. The finite element method reported in [34] has been used for the study.

The projections of the point displacement inside the finite element (u, v, w) can be represented as the product of the row vector of N^{T} shape functions and the corresponding nodal displacement column vectors u, v, w:

$$\mathrm{u} = \mathrm{N}^{\mathrm{T}}\mathrm{u}, \quad \mathrm{v} = \mathrm{N}^{\mathrm{T}}\mathrm{v}, \quad \mathrm{w} = \mathrm{N}^{\mathrm{T}}\mathrm{w}. \tag{9}$$

The strain equation for the three-dimensional case under consideration has the form:

$$\varepsilon = \begin{Bmatrix} \varepsilon_x \\ \varepsilon_y \\ \varepsilon_z \\ \gamma_{xy} \\ \gamma_{xz} \\ \gamma_{yz} \end{Bmatrix} = \begin{Bmatrix} \frac{\partial u}{\partial x} \\ \frac{\partial v}{\partial y} \\ \frac{\partial w}{\partial z} \\ \frac{\partial u}{\partial y} + \frac{\partial v}{\partial x} \\ \frac{\partial u}{\partial z} + \frac{\partial w}{\partial x} \\ \frac{\partial v}{\partial z} + \frac{\partial w}{\partial y} \end{Bmatrix} = \begin{bmatrix} \frac{\partial}{\partial x}\mathrm{N}^{\mathrm{T}} & 0 & 0 \\ 0 & \frac{\partial}{\partial y}\mathrm{N}^{\mathrm{T}} & 0 \\ 0 & 0 & \frac{\partial}{\partial z}\mathrm{N}^{\mathrm{T}} \\ \frac{\partial}{\partial y}\mathrm{N}^{\mathrm{T}} & \frac{\partial}{\partial x}\mathrm{N}^{\mathrm{T}} & 0 \\ \frac{\partial}{\partial z}\mathrm{N}^{\mathrm{T}} & 0 & \frac{\partial}{\partial x}\mathrm{N}^{\mathrm{T}} \\ 0 & \frac{\partial}{\partial z}\mathrm{N}^{\mathrm{T}} & \frac{\partial}{\partial y}\mathrm{N}^{\mathrm{T}} \end{bmatrix} \begin{Bmatrix} \mathrm{u} \\ \mathrm{v} \\ \mathrm{w} \end{Bmatrix}, \tag{10}$$

where $\varepsilon_x, \varepsilon_y, \varepsilon_z$ are the strain along the x, y, z axes;

$\gamma_{xy}, \gamma_{xz}, \gamma_{yz}$ are the strain tensors.

The stress equation for the considered three-dimensional case has the form:

$$\sigma = \begin{Bmatrix} \sigma_x \\ \sigma_y \\ \sigma_z \\ \tau_{xy} \\ \tau_{xz} \\ \tau_{yz} \end{Bmatrix} = G \begin{bmatrix} \gamma+1 & \gamma-1 & \gamma-1 & 0 & 0 & 0 \\ \gamma-1 & \gamma+1 & \gamma-1 & 0 & 0 & 0 \\ \gamma-1 & \gamma-1 & \gamma+1 & 0 & 0 & 0 \\ 0 & 0 & 0 & 1 & 0 & 0 \\ 0 & 0 & 0 & 0 & 1 & 0 \\ 0 & 0 & 0 & 0 & 0 & 1 \end{bmatrix} \begin{Bmatrix} \varepsilon_x \\ \varepsilon_y \\ \varepsilon_z \\ \gamma_{xy} \\ \gamma_{xz} \\ \gamma_{yz} \end{Bmatrix}, \quad (11)$$

where $\sigma_x, \sigma_y, \sigma_z$ are the stress along the x, y, z axes;

$\tau_{xy}, \tau_{xz}, \tau_{yz}$ are the stress tensors along the xy, xz, yz axes;

G is the modulus of elasticity of the floor material in shear;

$$G = \frac{E}{2(1+\mu)};$$

E is the modulus of elasticity of the blind floor material in tension;

$$\gamma = \frac{1}{1-2\mu};$$

μ is the Poisson's ratio of the blind floor material.

3. Results and Discussion

3.1. The Form of the Blind Floor of the All-Metal Gondola Car

Based on the criteria (7), (8) and the design features of the all-metal gondola car, as a result of numerous iterations on the stepped functions, the following form of the blind floor of the all-metal gondola car was obtained (Figure 3).

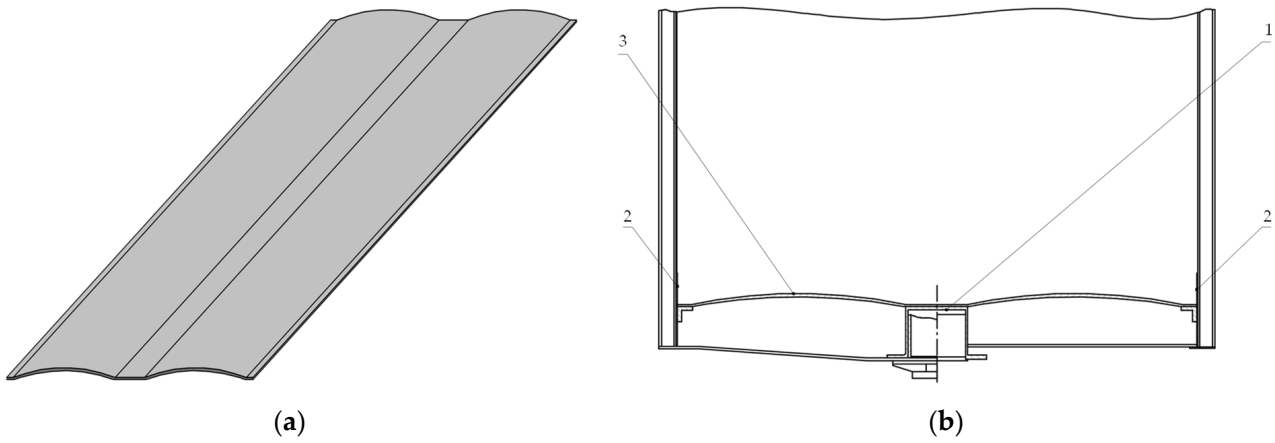

Figure 3. (**a**) The form of a blind floor; (**b**) the cross section of an all-metal gondola car with a blind floor: (1) Spinal beam; (2) bottom side panel; (3) blind floor.

The curvature of the blind floor (3) of Figure 3 should provide a simultaneous increase in the area, moments of inertia and a decrease in the weight of the body of an all-metal gondola car. The convexity of the blind floor of the all-metal gondola car allows increasing the strength.

The margin of safety of the blind floor was used to reduce the weight of the body of an all-metal gondola car.

Changing the shape of the blind floor at the same value of the allowable stress allows you to reduce the thickness of the blind floor of an all-metal gondola car. In a typical all-metal gondola car, the thickness of the blind floor is 6 mm or more. The blind floor of a typical all-metal gondola car is made of low-alloy steel 09G2S.

In the design of an all-metal gondola car with a blind floor (Figure 3b), cross-beams (4) of Figure 1 were removed. This makes it possible to further reduce the weight of an all-metal gondola car with a blind floor.

3.2. The Results of the Study of the Strength of the Blind Floor of an All-Metal Gondola Car

For strength studies, a universal four-axle, an all-metal gondola car with a blind floor, model 12-7019 (Ukraine), has been chosen. An all-metal gondola car model 12-7019 is designed for transportation of bulk cargoes that do not require protection from atmospheric precipitation on the railway network with a gauge of 1520 mm. The carrying capacity of an all-metal gondola car model 12-7019 is 72.0 tons.

The blind floor in an all-metal gondola car model 12-7019 is made according to the shape, as shown in Figure 3. The blind floor material is ordinary carbon steel. The thickness of the blind floor is 4–6 mm.

For research, a CAD model of a blind floor of an all-metal gondola car has been created. To solve the problem by the finite element method, the blind floor of an all-metal gondola car has been loaded with a distributed load of 80 kN. The load value of 80 kN has been chosen from the condition of overloading an all-metal gondola car by more than 10%.

Figure 4 shows the results of the equivalent stresses of the blind floor of an all-metal gondola car with a distributed load of 80 kN.

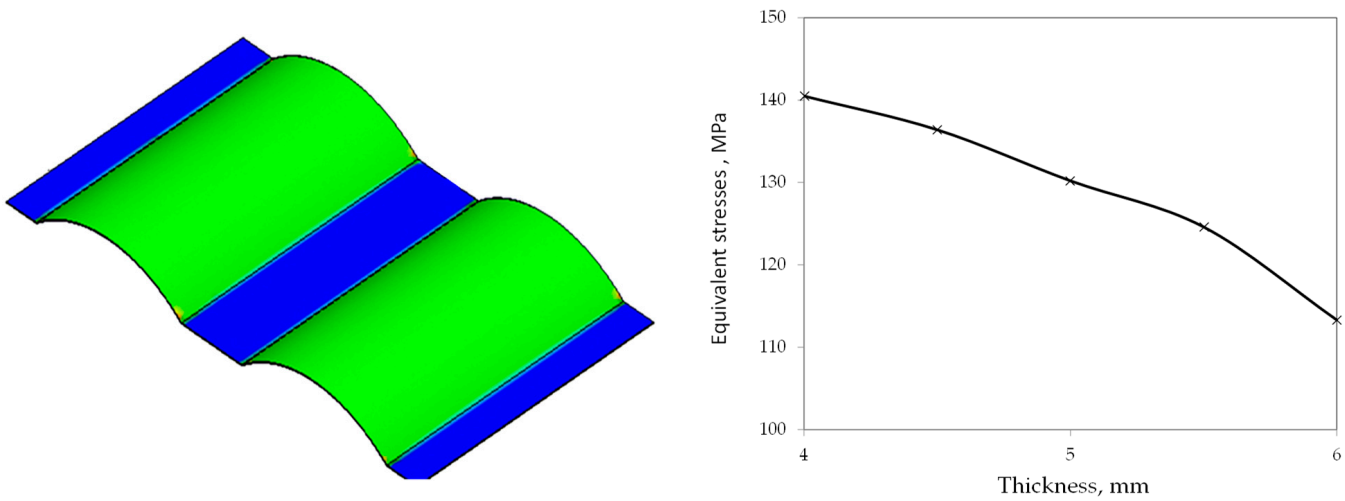

(**a**) (**b**)

Figure 4. (**a**) Equivalent stresses of the blind floor, 4 mm thickness; (**b**) distribution of maximum equivalent stresses in the blind floor of an all-metal gondola car in thickness.

Figure 5 shows the results of equivalent strains of the blind floor of an all-metal gondola car with a distributed load of 80 kN.

The results of equivalent stresses and strains of the blind floor of an all-metal gondola car (Figures 4 and 5) allow us to state that there is the margin of safety with a coefficient of 1.57–1.94, depending on the thickness of the blind floor.

The weight of an all-metal gondola car, model 12-7019, before changing the form of the blind floor of 6 mm is 22.0 tons. The change in the weight of an all-metal gondola car depending on the thickness of the blind floor is shown in Figure 6.

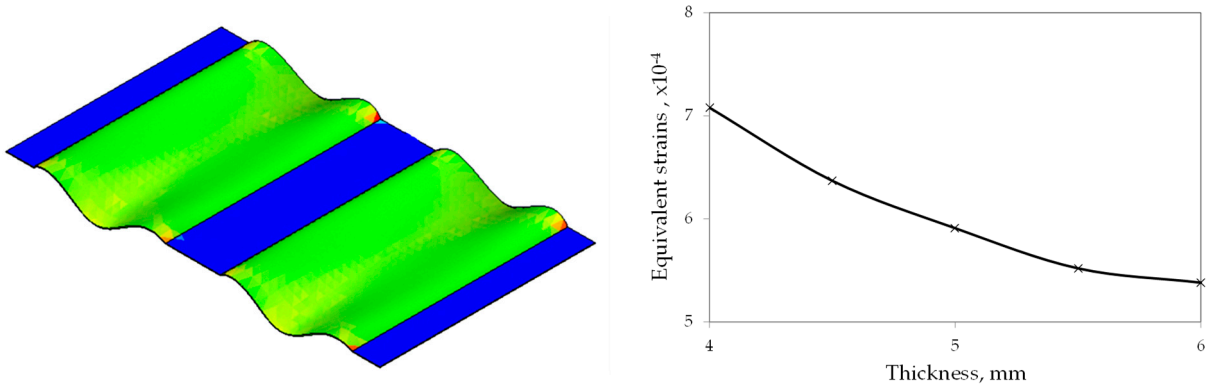

(**a**) (**b**)

Figure 5. (**a**) Equivalent strains of the blind floor, 4 mm thickness; (**b**) distribution of maximum equivalent strains in the blind floor of an all-metal gondola car over the thickness.

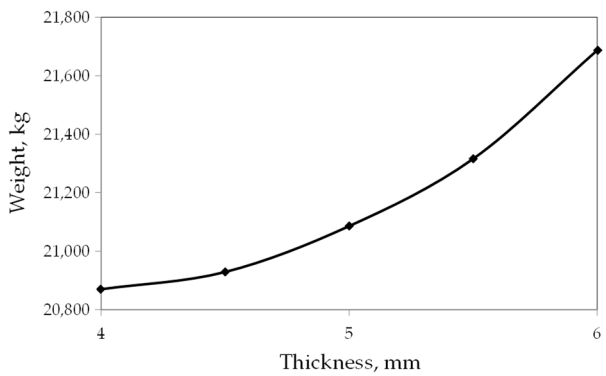

Figure 6. Weight of an all-metal gondola car, depending on the thickness of the blind floor.

3.3. Traction Energy Consumption

For an all-metal gondola car with a modified form of a blind floor, a comparison was made of the operating traction energy consumption. In this case, criterion (4) and its solution (5) have been used.

The estimate of the operating costs of the train delivery has been based on the calculation of the traction energy consumption. The train has been included of 40 all-metal gondola cars.

The comparison has been carried out for a typical all-metal gondola car and all-metal gondola car with a modified form of a blind floor.

The main data of the train considered for the calculation of the traction energy consumption are shown in Table 1.

Table 1. The main data of the train considered for the calculation of the traction energy consumption.

The Main Data	Units	Value
The length of the train section	km	200
The interval of train running time on the train section, which consisted of loaded all-metal gondola cars	minutes	190–340
The interval of train running time on the train section, which consisted of empty all-metal gondola cars	minutes	170–310

Traction locomotive has been electric locomotive VL-80t.

During the calculations, the parameters of the train section (longitudinal track profile and section plan), train parameters (weight, length and parameters of the braking system

of all-metal gondola cars), locomotive parameters (traction restrictions) and the interval of train running time on the train section have been taken into account.

The reduction in traction energy consumption when comparing the train with a typical all-metal gondola car and all-metal gondola car with a modified form of a blind floor, 4 mm thickness, is shown graphically in Figure 7.

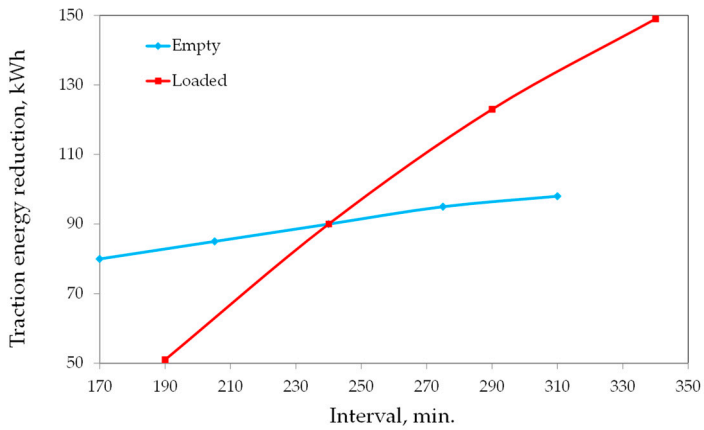

Figure 7. Reduction in traction energy consumption when comparing the train with a typical all-metal gondola car and all-metal gondola car with a modified form of a blind floor, 4 mm thickness, depending on the interval of train running time.

A decrease in the weight of an all-metal gondola car with a blind floor allows reducing the traction energy consumption. So, for a train with empty all-metal gondola cars with a modified form of a blind floor, the reduction in traction energy consumption was 79–98 kWh; for a train with loaded all-metal gondola cars with a modified form of a blind floor, the reduction in traction energy consumption was 51–149 kWh, depending on the interval of train running time.

4. Conclusions

In order to reduce the traction energy consumption, it has been proposed to decrease the weight of an all-metal gondola car with a blind floor.

Based on the developed criteria (7), (8), as a result of numerous iterations on the functions of the step type and when calculating the maximum stress (6), a new form of a blind floor has been obtained (Figure 3). As a result, an all-metal gondola car with a modified form of a blind floor has been obtained (Figure 3), which is characterized by a lower weight. The weight of an all-metal gondola car with a modified form of a blind floor, 4 mm thickness, was 5.1% less compared to a typical all-metal gondola car (Figure 6).

This paper studied the strength of an all-metal gondola car with a modified form of a blind floor (Figures 4 and 5). The equivalent stresses of a blind floor, 4 mm thickness (Figure 4), were 140.6 MPa with an allowable stress of 220 MPa. The margin of safety factor was 1.57. The equivalent strains of a blind floor, 4 mm thickness (Figure 5), were 7.08×10^{-4}, which is a low value for strain.

For an all-metal gondola car with a modified form of a blind floor, 4 mm thickness, a calculation has been made of reducing the traction energy consumption when compared with typical all-metal gondola cars with a blind floor.

The results of calculations of reducing traction energy consumption (Figure 7) showed that decreasing the weight of all-metal gondola cars with a modified form of a blind floor can reduce the traction energy consumption for loaded trains by 2.4–7.3% on the interval of train running time of 190–340 min, and for empty trains, by 2.5–3.1% on the interval of train running time of 170–310 min.

Thus, the performed study and a set of calculations confirmed the rationale for the use of an all-metal gondola car with a modified form of a blind floor to reduce the traction energy consumption.

The practical implementation of the project to introduce an all-metal gondola car with a modified form of a blind floor is scheduled for early 2024. The project implementation period is 1 year.

An analysis of emissions and socio-economic costs, which is given in [52], could also be carried out for this work in a similar way.

Author Contributions: Conceptualization, M.B. and O.B.; methodology, M.B.; software, L.K.; validation, A.B. and S.M.; formal analysis, O.B.; investigation, M.B.; resources, S.M.; writing—original draft preparation, M.B., L.K., O.B., A.B. and S.M.; writing—review and editing, M.B.; visualization, O.B.; supervision, M.B. All authors have read and agreed to the published version of the manuscript.

Funding: This research received no external funding.

Data Availability Statement: Not applicable.

Conflicts of Interest: The authors declare no conflict of interest.

References

1. Baranovskyi, D.; Muradian, L.; Bulakh, M. The Method of Assessing Traffic Safety in Railway Transport. In *IOP Conference Series: Earth and Environmental Science*; IOP Publishing: Bristol, UK, 2021; Volume 042075, pp. 1–6.
2. Shvets, A.O. Dynamic indicators influencing design solution for modernization of the freight rolling stock. *FME Trans.* **2021**, *49*, 673–683. [CrossRef]
3. Su, S.; Tang, T.; Wang, Y. Evaluation of Strategies to Reducing Traction Energy Consumption of Metro Systems Using an Optimal Train Control Simulation Model. *Energies* **2016**, *9*, 105. [CrossRef]
4. Andryushchenko, A.; Kolpahchyan, P.; Zarifyan, A. Reduction of electric locomotive's energy consumption by scalable tractive power control. *Transp. Probl.* **2018**, *13*, 103–110. [CrossRef]
5. Huang, Y.; Yang, L.; Tang, T.; Gao, Z.; Cao, F.; Li, K. Train speed profile optimization with on-board energy storage devices: A dynamic programming based approach. *Comput. Ind. Eng.* **2018**, *126*, 149–164. [CrossRef]
6. Baranovskyi, D.; Myamlin, S.; Podosonov, D.; Muradian, L. Determination of the filler concentration of the composite material to reduce the wear of the central bowl of the rail truck bolster. *Ain Shams Eng. J.* **2023**, 102232. [CrossRef]
7. Baranovskyi, D.; Myamlin, S. The criterion of development of processes of the self-organization of subsystems of the second level in tribosystems of diesel engine. *Sci. Rep.* **2023**, *13*, 5736. [CrossRef]
8. Gao, Z.; Yang, L. Energy-saving operation approaches for urban rail transit systems. *Front. Eng. Manag.* **2019**, *6*, 139–151. [CrossRef]
9. Zhang, R.; Yin, S.; Ye, M.; Yang, Z.; He, S. A Timetable Optimization Model for Urban Rail Transit with Express/Local Mode. *J. Adv. Transp.* **2021**, *2021*, 5589185. [CrossRef]
10. Yildiz, A.; Arikan, O.; Keskin, K. Traction energy optimization considering comfort parameter: A case study in Istanbul metro line. *Electr. Power Syst. Res.* **2023**, *218*, 109196. [CrossRef]
11. Shang, F.; Zhan, J.; Chen, Y. Energy-Saving Train Regulation for Metro Lines Using Distributed Model Predictive Control. *Energies* **2020**, *13*, 5483. [CrossRef]
12. Su, S.; Wang, X.; Cao, Y.; Yin, J. An Energy-Efficient Train Operation Approach by Integrating the Metro Timetabling and Eco-Driving. *IEEE Trans. Intell. Transp. Syst.* **2019**, *21*, 4252–4268. [CrossRef]
13. Baranovskyi, D.; Bulakh, M.; Myamlin, S.; Kebal, I. New Design of the Hatch Cover to Increase the Carrying Capacity of the Gondola Car. *Adv. Sci. Technol. Res. J.* **2022**, *16*, 186–191. [CrossRef]
14. Wang, X.; Xiao, Z.; Chen, M.; Sun, P.; Wang, Q.; Feng, X. Energy-Efficient Speed Profile Optimization and Sliding Mode Speed Tracking for Metros. *Energies* **2020**, *13*, 6093. [CrossRef]
15. He, D.; Yang, Y.; Chen, Y.; Deng, J.; Shan, S.; Liu, J.; Li, X. An integrated optimization model of metro energy consumption based on regenerative energy and passenger transfer. *Appl. Energy* **2020**, *264*, 114770. [CrossRef]
16. He, D.; Zhang, L.; Guo, S.; Chen, Y.; Shan, S.; Jian, H. Energy-efficient train trajectory optimization based on improved differential evolution algorithm and multi-particle model. *J. Clean. Prod.* **2021**, *304*, 127163. [CrossRef]
17. Liu, W.; Tang, T.; Su, S.; Yin, J.; Cao, Y.; Wang, C. Energy-Efficient Train Driving Strategy with Considering the Steep Downhill Segment. *Processes* **2019**, *7*, 77. [CrossRef]
18. Baranovskyi, D.; Myamlin, S.; Bulakh, M.; Podosonov, D.; Muradian, L. Determination of the Filler Concentration of the Composite Tape. *Appl. Sci.* **2022**, *12*, 11044. [CrossRef]
19. Rocha, A.; Araújo, A.; Carvalho, A.; Sepulveda, J. A New Approach for Real Time Train Energy Efficiency Optimization. *Energies* **2018**, *11*, 2660. [CrossRef]
20. Lingaitis, L.P.; Mjamlin, S.; Baranovsky, D.; Jastremskas, V. Experimental Investigations on Operational Reliability of Diesel Locomotyves Engines. *Eksploat. I Niezawodn. Maint. Reliab.* **2012**, *14*, 6–11.
21. Mazurkow, A.; Witkowski, W.; Kalina, A.; Wierzba, B.; Oleksy, M. The efect of oil feeding type and oil grade on the oil film bearing capacity. *Eksploat. I Niezawodn. Maint. Reliab.* **2021**, *23*, 381–386. [CrossRef]

22. Lingaitis, L.P.; Mjamlin, S.; Baranovsky, D.; Jastremskas, V. Prediction methodology of durability of locomotives diesel engines. *Eksploat. I Niezawodn. Maint. Reliab.* **2012**, *14*, 154–159.
23. Pu, Q.; Zhu, X.; Liu, J.; Cai, D.; Fu, G.; Wei, D.; Sun, J.; Zhang, R. Integrated optimal design of speed profile and Fuzzy PID controller for train with multifactor consideration. *IEEE Access* **2020**, *8*, 152146–152160. [CrossRef]
24. Chmielowiec, A. Algorithm for error-free determination of the variance of all contiguous subsequences and fixed-length contiguous subsequences for a sequence of industrial measurement data. *Comput. Stat.* **2021**, *36*, 2813–2840. [CrossRef]
25. Chmielowiec, A.; Litwin, P. Efficient Inverted Index Compression Algorithm Characterized by Faster Decompression Com-pared with the Golomb-Rice Algorithm. *Entropy* **2021**, *23*, 296. [CrossRef] [PubMed]
26. Douglas, H.; Roberts, C.; Hillmansen, S.; Schmid, F. An assessment of available measures to reduce traction energy use in railway networks. *Energy Convers. Manag.* **2015**, *106*, 1149–1165. [CrossRef]
27. Kalina, A.; Mazurkow, A.; Witkowski, W.; Wierzba, B.; Oleksy, M. Properties of elasto-hydrodynamic oil film in meshing of harmonic drive gears. *Materials* **2021**, *14*, 1194. [CrossRef] [PubMed]
28. Baranovskyi, D.; Bulakh, M.; Michajłyszyn, A.; Myamlin, S.; Muradian, L. Determination of the Risk of Failures of Locomotive Diesel Engines in Maintenance. *Energies* **2023**, *16*, 4995. [CrossRef]
29. Montrone, T.; Pellegrini, P.; Nobili, P. Real-time energy consumption minimization in railway networks. *Transp. Res. Part D Transp. Environ.* **2018**, *65*, 524–539. [CrossRef]
30. Tian, Z.; Zhao, N.; Hillmansen, S.; Roberts, C.; Dowens, T.; Kerr, C. SmartDrive: Traction Energy Optimization and Applications in Rail Systems. *IEEE Trans. Intell. Transp. Syst.* **2019**, *20*, 2764–2773. [CrossRef]
31. Blanco-Castillo, M.; Fernández-Rodríguez, A.; Fernández-Cardador, A.; Cucala, A.P. Eco-Driving in Railway Lines Considering the Uncertainty Associated with Climatological Conditions. *Sustainability* **2022**, *14*, 8645. [CrossRef]
32. Tupaj, M.; Orłowicz, A.W.; Mróz, M.; Trytek, A.; Dolata, A.J.; Dziedzic, A. A Study on Material Properties of Intermetallic Phases in a Multicomponent Hypereutectic Al-Si Alloy with the Use of Nanoindentation Testing. *Materials* **2020**, *13*, 5612. [CrossRef] [PubMed]
33. Kida, M.; Koszelnik, P. Investigation of the Presence and Possible Migration from Microplastics of Phthalic Acid Esters and Polycyclic Aromatic Hydrocarbons. *J. Polym. Environ.* **2020**, *29*, 599–611. [CrossRef]
34. Zhang, D.; Tang, Y.; Peng, Q.; Dong, C.; Ye, Y. Effect of mass distribution on curving performance for a loaded wagon. *Nonlinear Dyn.* **2021**, *104*, 2259–2273. [CrossRef]
35. Sandrini, G.; Gadola, M.; Chindamo, D.; Candela, A.; Magri, P. Exploring the Impact of Vehicle Lightweighting in Terms of Energy Consumption: Analysis and Simulation. *Energies* **2023**, *16*, 5157. [CrossRef]
36. Zhang, W.; Xu, J. Advanced lightweight materials for Automobiles: A review. *Mater. Des.* **2022**, *221*, 110994. [CrossRef]
37. Deepati, A.K.; Alhazmi, W.; Benjeer, I. Mechanical characterization of AA5083 aluminum alloy welded using resistance spot welding for the lightweight automobile body fabrication. *Mater. Today Proc.* **2021**, *45*, 5139–5148. [CrossRef]
38. Sateesh, N.; Subbiah, R.; Nookaraju, B.; Nagaraju, D.S. Achieving safety and weight reduction in automobiles with the application of composite material. *Mater. Today Proc.* **2022**, *62*, 4469–4472. [CrossRef]
39. Czerwinski, F. Current Trends in Automotive Lightweighting Strategies and Materials. *Materials* **2021**, *14*, 6631. [CrossRef]
40. Ulianov, C.; Önder, A.; Peng, Q. Analysis and selection of materials for the design of lightweight railway vehicles. In *IOP Conference Series: Materials Science and Engineering*; IOP Publishing: Bristol, UK, 2018; Volume 292, p. 012072. [CrossRef]
41. Özdemir, A.; Önder, A. An environmental life cycle comparison of various sandwich composite panels for railway passenger vehicle applications. *Environ. Sci. Pollut. Res.* **2020**, *27*, 45076–45094. [CrossRef]
42. Słowiński, M. An Analysis of CFRP Application in the Construction of Rail Vehicles. *Probl. Kolejnictwa Railw. Rep.* **2021**, *65*, 105–113. [CrossRef]
43. Mistry, P.; Johnson; Galappaththi, U. Selection and ranking of rail vehicle components for optimal lightweighting using composite materials. *Proc. Inst. Mech. Eng. Part F J. Rail Rapid Transit* **2020**, *235*, 390–402. [CrossRef]
44. Winnett, J.; Hoffrichter, A.; Iraklis, A.; McGordon, A.; Hughes, D.J.; Ridler, T.; Mallinson, N. Development of a very light rail vehicle. In Proceedings of the Institution of Civil Engineers Transpor; Thomas Telford Ltd.: London, UK, 2017; pp. 231–242.
45. Galimova, F.; Khurmatov, Y.; Abdulloev, M.; Jumabekov, B.; Sultonaliev, D.; Ergeshova, D. Modern Gondola with Lightweight Body. In *XIV International Scientific Conference "INTERAGROMASH 2021"*; Springer: Berlin/Heidelberg, Germany, 2022; pp. 1043–1050. [CrossRef]
46. Panchenko, S.; Gerlici, J.; Vatulia, G.; Lovska, A.; Ravlyuk, V.; Harusinec, J. Studying the load of composite brake pads under high-temperature impact from the rolling surface of wheels. *EUREKA Phys. Eng.* **2023**, *4*, 155–167. [CrossRef]
47. Popov, E.S.; Shinsky, O.I. Performance quality analysis of brake iron and composite pads for railway rolling composition. *Litiyo i Met. (Foundry Prod. Met.)* **2021**, *1*, 27–37. [CrossRef]
48. Robinson, M.; Carruthers, J.; O'Neill, C.; Ingleton, S.; Grasso, M. Transport of DE-LIGHT: The design and prototyping of a light-weight crashworthy rail vehicle driver's cab. *Procedia-Soc. Behav. Sci.* **2012**, *48*, 672–681. [CrossRef]
49. Mistry, P. Johnson Lightweighting of railway axles for the reduction of unsprung mass and track access charges. *Proc. Inst. Mech. Eng. Part F J. Rail Rapid Transit* **2020**, *234*, 958–968. [CrossRef]
50. Bruni, S.; Mistry, P.J.; Johnson, M.S.; Bernasconi, A.; Carboni, M.; Formaggioni, D.; Carra, G.; Macchiavello, S.; Ferrante, E.; Kaiser, I.; et al. A vision for a lightweight railway wheelset of the future. *Proc. Inst. Mech. Eng. Part F J. Rail Rapid Transit* **2022**, *236*, 1179–1197. [CrossRef]

51. Mistry, P.J.; Johnson, M.S.; Li, S.; Bruni, S.; Bernasconi, A. Parametric sizing study for the design of a lightw eight composite railway axle. *Compos. Struct.* **2021**, *267*, 113851. [CrossRef]
52. Cecchel, S.; Chindamo, D.; Turrini, E.; Carnevale, C.; Cornacchia, G.; Gadola, M.; Panvini, A.; Volta, M.; Ferrario, D.; Golimbioschi, R. Impact of reduced mass of light commercial vehicles on fuel consumption, CO_2 emissions, air quality, and socio-economic costs. *Sci. Total. Environ.* **2018**, *613–614*, 409–417. [CrossRef]

Disclaimer/Publisher's Note: The statements, opinions and data contained in all publications are solely those of the individual author(s) and contributor(s) and not of MDPI and/or the editor(s). MDPI and/or the editor(s) disclaim responsibility for any injury to people or property resulting from any ideas, methods, instructions or products referred to in the content.